Thrust Control of Traction Linear Induction Motors in Switch Areas

Cai-Xia Tao,Dan Zhang,Xiao Li
School of Automation and Electrical engineering Lanzhou JiaoTong University
88 West Anning Rd.Lanzhou Gansu
China
02130418@stu.lzjtu.edu.cn http://mail.lzjtu.edu.cn/

Abstract: Rail transit systems powered by linear induction motors have gained widespread popularity. In order to solve the problem of no thrust in switch areas where there are no sensor boards, the motor thrust is increased prior to entering the switch area so that the total thrust remains constant. In the two conditions,where include and exclude secondary,not only the linear induction motor models was established, but also the simulation models of the direct thrust control and the constant thrust control were established. Simulation studies were conducted on the direct thrust of a single motor, and the constant thrust control of the train.Experimental results have validated the models.

Keywords: rail transit system;linear induction; motor;direct thrust control;switch area;prior;secondary

1 Introduction

With the increasingly serious problem of urban traffic congestion, China has entered a peak period of urban rail transit development.Trains with single sided linear induction motors have the advantages of fast acceleration,high climbing ability, and small turning radius;requiring small areas of tunnel structures and providing more flexible choices of subway lines. Therefore, rail transport systems powered by linear induction motors have gained widespreed attention[1]. Direct thrust control control technology has simple algorithms,fast dynamic response, robustness against parameter variations, and is ideal for controlling traction motor[2]. A great deal of research has been conducted on single sided linear induction motors. The impact of the second longitudinal edge effect on motor class electromagnetic force is analyzed by solving the motor air gap magnetic field distribution[3]. No unit dimension of Q is introduced to amend the secondary resistance and mutual inductance in the rotary induction motors[4]. Slip-frequency scalar control mode is widely used for linear induction motor control in urban rail systems[5].Direct thrust control based on a switch table is simulated in[6]. The direct thrust control of efficiency optimization energy-saving control is applied to curved linear induction motors.It is obviously illustrated that linear induction motor trains will lose thrust in switch areas.In spite of extensive studies, no solution has been found to the problem of loss of thrust in switch areas of non induction.

For the thrust loss problem, this paper creates a model of linear induction motors without secondary plate situation in a stationary coordinate system. The simulation models of linear induction traction motors and direct thrust are built in Matlab/Simulink. The simulation of speed control and thrust control is conducted to verify the control system. Furthermore, the constant thrust control in switch areas is analyzed and the future research work is discussed.

2 Mathematical model of linear induction motor

Linear induction motors can be considered as the rotary induction motor sectioned axially and

expanded horizontally. The stator on the motor frame becomes the primary on the bottom of the train, and the rotor becomes the secondary laid in the middle of the rails. This asymmetry causes the edge effect, and the second longitudinal edge effect is the most significant. Given the correction factor of the second longitudinal edge effect Q[7].

$$Q = \frac{T_v}{T_r} = \frac{DR_r}{(L_m + L_r)v} \tag{1}$$

Where, T_v is the constant of primary time, T_r is the constant of secondary time, R_r is secondary resistance, L_m is the mutual inductance, L_r is the secondary leakage inductance, D is the primary length, v is the speed.

Edge effect function is[7]:

$$f(Q) = \frac{1 - e^{-Q}}{Q} \tag{2}$$

Eddy-current loss is equivalent to the variation of the excitation resistance at the ends of the secondary. The revised excitation resistance is[7]:

$$R_r^{'} = R_r f(Q) \tag{3}$$

The demagnetization effect of a secondary vortex is equivalent to the variation of magnetic inductance. The revised magnetic inductance is[7]:

$$L_m^{'} = L_m[1 - f(Q)] \tag{4}$$

Where , $L_m^{'}$ is excitation inductance which corrected, $R_r^{'}$ is the excitation resistance which corrected.

The equivalent circuit of a linear induction motor with the second longitudinal edge effect is shown in Fig.1, where R_s is the primary resistance, L_s is the primary leakage inductance, u s is the primary voltage vector, I_s is the primary current vector, I_r is the secondary current vector, and I_m is the mutual inductance of the current vector.

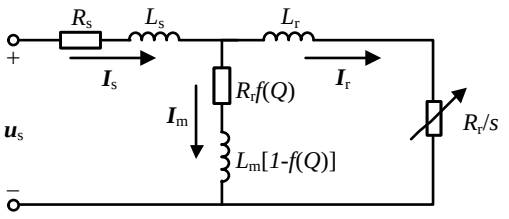

Fig. 1 Linear induction motor equivalent circuit

Based on the equivalent circuit of Fig.1, a dynamic mathematical model of linear inducttion motors in two-phase stationary αβ coordinate system is built as follows. The voltage equation is:

$$\begin{cases} u_{s\alpha} = R_s i_{s\alpha} + R_r^{'}(i_{s\alpha} + i_{r\alpha}) + \dfrac{d\psi_{s\alpha}}{dt} \\ u_{s\beta} = R_s i_{s\beta} + R_r^{'}(i_{s\beta} + i_{r\beta}) + \dfrac{d\psi_{s\beta}}{dt} \\ 0 = R_r i_{r\alpha} + R_r^{'}(i_{s\alpha} + i_{r\alpha}) + \dfrac{d\psi_{r\alpha}}{dt} + \omega_r \psi_{r\beta} \\ 0 = R_r i_{r\beta} + R_r^{'}(i_{s\beta} + i_{r\beta}) + \dfrac{d\psi_{r\beta}}{dt} - \omega_r \psi_{r\alpha} \end{cases} \tag{5}$$

Where, $u_{s\alpha}$ is the α-axis primary voltage, $u_{s\beta}$ is the β-axis primary voltage, $i_{s\alpha}$ is the α-axis primary current, $i_{s\beta}$ is the β-axis primary current, $i_{r\alpha}$ is the α-axis secondary current, $i_{r\beta}$ is the β-axis secondary current, $\psi s\alpha$ is the α-axis primary flux, $\psi_{s\beta}$ is the β-axis primary flux; $\psi_{r\alpha}$ is the α-axis secondary flux, $\psi_{r\beta}$ is the β-axis secondary flux, and ω_r is the linear induction motor equivalent angular velocity.

The flux equation is:

$$\begin{cases} \psi_{s\alpha} = L_s i_{s\alpha} + L_m^{'}(i_{s\alpha} + i_{r\alpha}) \\ \psi_{s\beta} = L_s i_{s\beta} + L_m^{'}(i_{s\beta} + i_{r\beta}) \\ \psi_{r\alpha} = L_r i_{r\alpha} + L_m^{'}(i_{s\alpha} + i_{r\alpha}) \\ \psi_{r\beta} = L_r i_{r\beta} + L_m^{'}(i_{s\beta} + i_{r\beta}) \end{cases} \tag{6}$$

The equation of motion is[8]:

$$F_e - F_{load} = m\frac{dv}{dt} \tag{7}$$

Where, F_e is the electromagnetic force, F_{load}, is the load thrust, and m is the primary quality.

The thrust equation is:

$$F_e = \frac{3\pi}{2\tau}\frac{p}{4}(\psi_{s\alpha} i_{s\beta} - \psi_{s\beta} i_{s\alpha}) \tag{8}$$

Simulink doesn't include a linear induction

motor model required in the simulation. We build a linear induction motor model using an s-function described as follows.

In order to obtain the equation of s-fuction, we calculate the current based on the flux equation of the linear induction motor.

$$\begin{cases} i_{s\alpha} = [L_m^{'}\psi_{r\alpha} - (L_r + L_m^{'})\psi_{s\alpha}]A^{-1} \\ i_{s\beta} = [L_m^{'}\psi_{r\beta} - (L_r + L_m^{'})\psi_{s\beta}]A^{-1} \\ i_{r\alpha} = [L_m^{'}\psi_{s\alpha} - (L_r + L_m^{'})\psi_{r\alpha}]A^{-1} \\ i_{r\beta} = [L_m^{'}\psi_{s\beta} - (L_r + L_m^{'})\psi_{r\beta}]A^{-1} \end{cases} \quad (9)$$

$$A = L_m^{'\,2} - (L_s + L_m^{'})(L_r + L_m^{'}) \quad (10)$$

The flux linkages state equation is obtained from the voltage equation of the linear induction motor.

$$\begin{cases} \frac{d\psi_{s\alpha}}{dt} = u_{s\alpha} - R_s i_{s\alpha} - R_r^{'}(i_{s\alpha} + i_{r\alpha}) \\ \frac{d\psi_{s\beta}}{dt} = u_{s\beta} - R_s i_{s\beta} - R_r^{'}(i_{s\beta} + i_{r\beta}) \\ \frac{d\psi_{r\alpha}}{dt} = -R_r i_{r\alpha} - R_r^{'}(i_{s\alpha} + i_{r\alpha}) - \omega_r \psi_{r\beta} \\ \frac{d\psi_{r\beta}}{dt} = -R_r i_{r\beta} - R_r^{'}(i_{s\beta} + i_{r\beta}) + \omega_r \psi_{r\alpha} \end{cases} \quad (11)$$

The angular velocity state equation is obtained from the angular velocity of movement[8]:

$$\frac{d\omega_r}{dt} = \frac{\pi}{m\tau}(F_e - F_{load}) \quad (12)$$

Linear induction motors don't have thrust in a switch area where the secondary sensor boards cannot be laid. In reality, inertia carries the train out of the switch area. In this case, other motors temporarily increase the thrust to compensate for the loss of thrust of the linear induction motors. In the switch areas of non-induction, the mathematical model of the linear induction motor needs to be modified to exclude the secondary. First calculate the mutual inductance, L_m is calculated as[9]:

$$L_m = \frac{4m_1}{\pi}\mu_0 \frac{(W_1 k_{w1})^2 2av_s}{2gk_g k_\mu \frac{(2p-1)^2}{4p-3}} \frac{1}{2\pi f} \quad (13)$$

$$k_{w1} = \frac{\sin(\frac{\pi}{2m_1})\sin(\beta_y 2\pi)}{q_1 \sin(\frac{\pi}{2m_1 q_1})} \quad (14)$$

$$k_g = \frac{t_1}{t_1 - \frac{b_0^2/g}{5 + b_0/g}} \quad (15)$$

Where, m_1 is the number of phase, μ_0 represents the vacuum permeability, W_1 is each series with the primary winding turns, kw_1 is the winding factor; k_g is the gap coefficient, k_μ is the magnetic saturation coefficient, β_y is the relative pitch of the winding; q_1 is the number of slots per pole per phase, t_1 is the primary pitch, and b_0 is the groove width.

From Equation 13, the mutual inductance is inversely proportional to the mechanical air gap of the linear induction motor. In the switch area of non-induction, the mechanical air gap is $g=\tau\pi$[9].

The mutual inductance was 0.64mH. Far less than the mutual inductance of linear induction motor with secondary 4.36mH, so the mutual inductance can be ignored. At the same time because only contain primary, so secondary parameters are ignored.

The flux linkages state equation is:

$$\begin{cases} \frac{\mathrm{d}\psi_{s\alpha}}{\mathrm{d}t} = u_{s\alpha s\,\bar{\alpha}} - R\,i \\ \frac{\mathrm{d}\psi_{s\beta}}{\mathrm{d}t} = u_{s\beta s\,\bar{\beta}} - R\,i \end{cases} \quad (16)$$

The current is calculated as:

$$\begin{cases} i_{s\alpha} = L_s^{-1}\psi_{s\alpha} \\ i_{s\beta} = L_s^{-1}\psi_{s\beta} \end{cases} \quad (17)$$

3 Direct Thrust Control Simulation Model

Direct Thrust Control and direct torque control are actually equivalent. The primary and the

secondary of linear induction motors do a relative linear motion. At this point the electromagnetic torque is the electromagnetic force. They can be converted between each other, namely[10]:

$$T_e = F_e \frac{p\tau}{2\pi} \tag{18}$$

Where, T_e, is electromagnetic torque.

The control block diagram of direct thrust based on the principle of switching vector table is shown in Figure 2. There are three components including the flux and thrust observer, the flux regulator, the thrust regulator and the switch table[11].

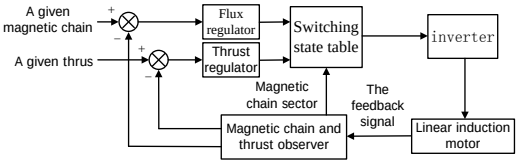

Fig.2 Direct Thrust Control Block Diagram

Compared with direct torque control,accurate flux observation of the linear induction motor is the key to improve the direct thrust control performance. The stator flux is obtained using the stator voltage and current in the rotary induction motor.

$$\begin{cases} \psi_{s\alpha} = \int [u_{s\alpha} - R_s i_{s\alpha}]dt \\ \psi_{s\beta} = \int [u_{s\beta} - R_s i_{s\beta}]dt \end{cases} \tag{19}$$

The edge effect needs to be considered when this stator flux model is applied to linear induction motors.

The above formulas are modified as:

$$\begin{cases} \psi_{s\alpha} = \int [u_{s\alpha} - R_s i_{s\alpha} - R_r^{'}(i_{s\alpha} + i_{r\alpha})]dt \\ \psi_{s\beta} = \int [u_{s\beta} - R_s i_{s\beta} - R_r^{'}(i_{s\beta} + i_{r\beta})]dt \end{cases} \tag{20}$$

Take Guangzhou Metro Line FOUR as an example. The train had four motor train units. Each unit had an inverter and two linear induction motors. Each inverter drove a motor as a simplified simulation model, totaling four motors. The amplitude of the primary current in the stationary coordinate system increases. The amplitude variation of the current is checked to decide when the motor is detached from the secondary sensor board, which is the timing of increasing the thrust before entering the switch area. Matlab/Simulink was used to build the model as shown in Fig.3.

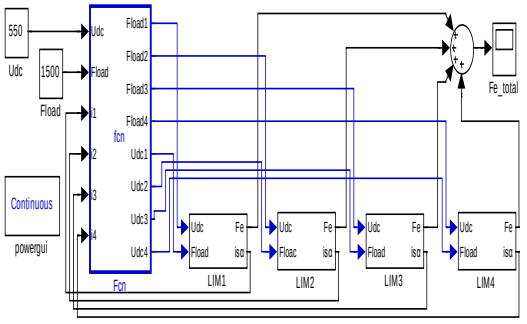

Fig.3 Simulation Model of Constant Thrust Control

The direct thrust control of a single linear induction motor model is shown in Fig.4.

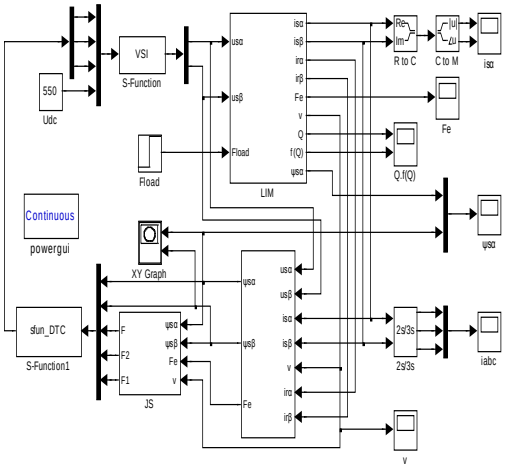

Fig.4 Direct thrust control model of a linear induction motor

4 Simulation Analysis

First, the direct thrust control of a single linear induction motor was simulated, where R_s was 0.045Ω, R_r was 0.126Ω, L_s was 1.21mH, L_r was 0.35mH, L_m was 4.36mH, p was 6, τ was 0.288, m was 500kg, and D was 1.732m. The speed PI regulator parameters K_P was 5000, and K_I was 175. The given flux value was 0.8Wb. The hysteresis flux linkage regulator loop width was 0.002Wb, and the thrust hysteresis regulator loop width was 0.05N. We used the simulation algorithm ode4, and simulation step was 10^{-5}s.

The speed step simulation conditions are that the speed at the beginning (0 second) was 8m/s, the speed at 2.5seconds was 10m/s, and the thrust load was 1000N. The speed response curve of the linear induction motor is shown in Figure 5. The three-phase current curve of the linear induction motor is shown in Figure 6. It is noted that with a constant speed the amplitude of the current increased as the speed increased. This is because the current needs to be increased to compensate the loss caused by the edge effect.

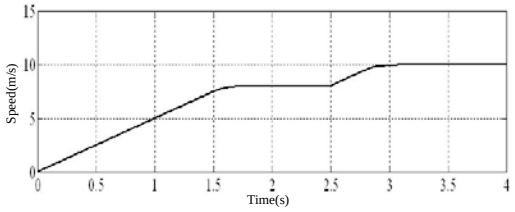

Fig.5 Speed waveform of a linear induction motor

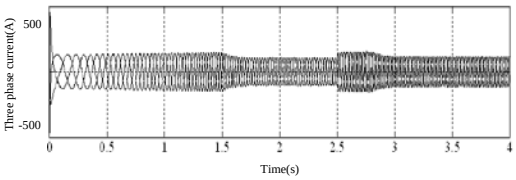

Fig.6 Tthree-phase current of a linear induction motor

The thrust step simulation conditions are that the load thrust was 1000N at the beginning and 2000N at 2.5 seconds, and the given speed was 8m/s. The wave of electromagnetic wave is shown in Fig.7, which can track the thrust.

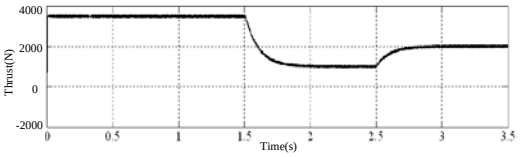

Fig.7 Electromagnetic thrust with edge effect

The simulation conditions of the linear induction motor without the secondary are that the given speed was 8m / s, and the load thrust was 1500N. Assume that the secondary was dispatched from the linear induction motor at 2.5seconds. The mutual inductance was 0.64m

H. The three-phase current waveform is shown in Fig.8. It was noted that the frequency of the three-phase current in the first linear induction motor dramatically increased in the time period from 2.5seconds to 3.5seconds. The α-axis three-phase current of the linear induction motor is shown in Fig.9, where the current amplitude rose to 440A which led to a 300% overload.

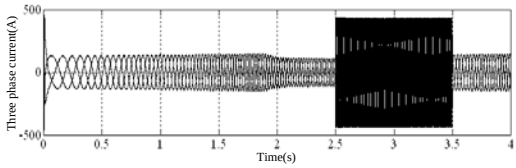

Fig.8 Three-phase current of the first linear induction motor

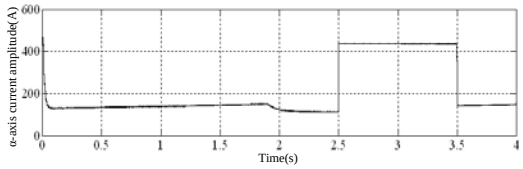

Fig.9 α-axis current amplitude of the first linear induction motor

Next, the constant thrust control of the model in Figure 3 was simulated. The α-axis current of the linear induction motor was investigated. When the current is 200% higher than normal, we increased the thrust of the other three motors by one third. The thrust of the first motor is shown in Fig.10. There were no sensor boards between 2.5 seconds and 3.5 seconds. The thrust of the second motor is shown in Fig.11. The thrust increased by one third between 2.5seconds to 3.5 seconds. The total thrust of the four motors is shown in Figure 12, which was a constant of 6000N between 2.5seconds to 3.5seconds. The slight drop after 2.5 seconds was due to the delay of the thrust boost of other three motors (second to fourth). There was one second speed loss when there was a thrust loss in the first motor, which caused the slight rise of the total thrust after 3.5seconds. After 3.5 seconds, the first motor operated normally producing full thrust and the train regained the given speed.

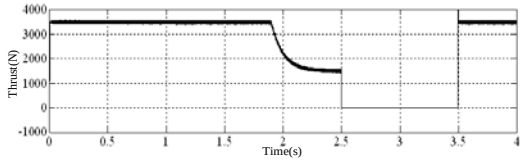

Fig.10 Thrust of the first linear induction motor

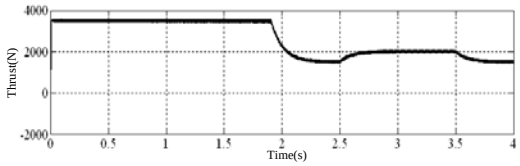

Fig.11 Thrust of the second linear induction motor

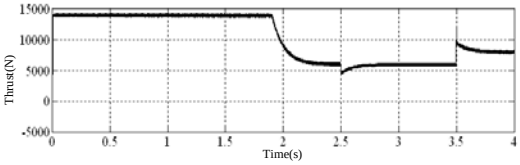

Fig.12 Total thrust of four linear induction motor

5 Conclusion

This paper established a mathematical model of linear induction motor in the two-phase stationary coordinate system using s-fuction.The direct thrust control strategy of linear induction motors was studied and simulated using Matlab/Simulink software.

The simulation results suggested the following:

The thrust of motors in the non-induction area dropped to zero. Constant total thrust was achieved by increasing the thrust of other motors. The timing for compensating thrust was determined by the variation of the α-axis primary current amplitude in the αβ coordinate system. The overload of the α-axisprimary current amplitude of the motor in a non-induction area was around 300%. The simulation was conducted of the thrust loss of one motor in the switch area. The strategy should be modified for practical situations, including the timing of thrust compensation and the overloading capability of each motor.

References:

[1] Gieras JF,Linera Induction drives,Oxford:Clarend on Press ,1994,pp.4-8.

[2] Depenbrock M,Direct self-control (DSC) of inver ter-fed induction machine ,IEEE Trans.On Power Electronics, Vol.3,No.4,1988,pp.420-429.

[3] Yamamura S,Theory of linear induction motors (second edition),Tokyo:University of TokyoPress, 1978,pp.35-37.

[4]Duncan J., Eng C,Linear induction motor equival ent-circuit model,IEEE Trans,On Electric Power Applications, Vol.130,No.1,1983,pp.51-57.

[5] Zheng Qiongling, Zhao Jia, and Fan Jiafen, Rail traction transmission of linear motor, China ScienceandTechnologyPress,Beijing,Vol.15,No. 19,2009,pp.60-62.

[6] Lai YS, Chen JH,A New Approach to Direct Torq ue Control of Induction Motor Drives for Consta nt Inverter Switching Frequency and Torque Ripple Reduction,IEEE Transactions on Energy Conversion, Vol.16,No.3,2001,pp.220-227.

[7] Wang Ke, City rail linear induction motor charact eristics analysis and direct traction control strateg y , Beijing: Institute of Electrical Engineering, 2009:44.

[8] Li Xiao, Tao Caixia, Finite element analysis of traction linear induction motor based on Ansoft Software,Study of urban rail traffic,Vol.17,No.3 ,2014,pp.79-82.

[9] Long Xialing,Theory of linear induction motors and electromagnetic design,Beijing:Science Press Vol.1,No.6,2006,pp.173-182.

[10]Marcello Pucci,State space-vector model of linea induction motors,IEEE Trans. On Industry Appl ications,Vol.50,No.1,2014 ,pp.195-207.

[11]LuQingfen, Characteristics of linear synchronous motors,Hangzhou:Zhejiang University,2005.